Drainage-structuring of ancestral variation and a common functional pathway shape limited genomic convergence in natural high- and low-predation guppies

Authors:

James R. Whiting[1] , Josephine R. Paris[1] , Mijke J. van der Zee[1], Paul J. Parsons[1,2] , Detlef Weigel[3], Bonnie A. Fraser[1]

Corresponding Author: Bonnie Fraser, b.fraser@exeter.ac.uk

Author Affiliations:

1) Department of Biosciences, University of Exeter, Stocker Road, Exeter EX4 4QD, UK
2) Department of Animal and Plant Sciences, University of Sheffield, Alfred Denny Building, University of Sheffield, Western Bank, Sheffield S10 2TN, UK
3) Department of Molecular Biology, Max Planck Institute for Developmental Biology, Max-Planck-Ring 5, 72076 Tübingen, Germany

Keywords:

Convergent evolution, genomic convergence, guppy, population genomics, adaptation

ABSTRACT

Studies of convergence in wild populations have been instrumental in understanding adaptation by providing strong evidence for natural selection. At the genetic level, we are beginning to appreciate that the re-use of the same genes in adaptation occurs through different mechanisms and can be constrained by underlying trait architectures and demographic characteristics of natural populations. Here, we explore these processes in naturally adapted high- (HP) and low-predation (LP) populations of the Trinidadian guppy, *Poecilia reticulata*. As a model for phenotypic change this system provided some of the earliest evidence of rapid and repeatable evolution in vertebrates; the genetic basis of which has yet to be studied at the whole-genome level. We collected whole-genome sequencing data from ten populations (176 individuals) representing five independent HP-LP river pairs across the three main drainages in Northern Trinidad. We evaluate population structure, uncovering several LP bottlenecks and variable between-river introgression that can lead to constraints on the sharing of adaptive variation between populations. Consequently, we found limited selection on common genes or loci across all drainages. Using a pathway type analysis, however, we find evidence of repeated selection on different genes involved in cadherin signalling. Finally, we found a large repeatedly selected haplotype on chromosome 20 in three rivers from the same drainage. Taken together, despite limited sharing of adaptive variation among rivers, we found evidence of convergent evolution associated with HP-LP environments in pathways across divergent drainages and at a previously unreported candidate haplotype within a drainage.

23 **INTRODUCTION**

24 The process of adaptation in nature can be thought of as a complex interplay between random
25 happenstance and repeatable processes in independent lineages. The latter of these, often
26 termed convergent or parallel evolution [1,2], has provided a myriad of examples from which
27 general rules and principles of adaptation have been dissected under natural conditions.
28 Empirical evidence accumulated over the last decade has demonstrated that convergent
29 phenotypes are often underwritten by convergent changes at the genetic level across many
30 taxa (reviewed in [3–6]). We are now at the point where we can ask why genetic convergence
31 ranges from common in some systems to non-existent in others.
32
33 While, there are many definitions of genetic convergence (or parallelism) [2], here we use it
34 broadly to describe selection acting at any of three levels: on the same mutations (eg. [7–9]);
35 different mutations in the same genes (eg. [10–12]); or different genes in the same functional
36 pathways (eg. [13–16]). Further, variation among lineages may arise through one of three
37 modes: either *de novo* mutations (eg. [17,18]); as shared ancestral variation (eg. [19,20]); or
38 through introgression among lineages (eg. [21–24]). An emerging trend within systems is that
39 adaptation involving multiple traits can involve combinations of these levels and modes of
40 convergence. For example, stickleback adapting to freshwater experience selection on ancestral
41 *eda* haplotypes [25] and *de novo* mutation at the *pitx1* gene [10] to repeatedly evolve
42 freshwater bony armour plate and pelvis phenotypes respectively. Similarly, Pease et al. [26]
43 found all three modes of convergence occurring across a clade of wild tomato accessions:
44 adaptive introgression of alleles associated with immunity to fungal pathogens, selection on an

ancestral allele conferring fruit colour, and repeated *de novo* mutation of alleles associated with seasonality and heavy metal tolerance. Further, the same phenotype may arise in response to the same selection through any of the above modes, as observed in glyphosate-resistance amaranths across North America [27]. In this study, the authors found glyphosate-resistance evolved in one location by introgression and selection on a pre-adapted allele, in another by the fixation of a shared ancestral haplotype, and in a third location through selection on multiple, derived haplotypes.

Given the range of genetic convergence observed across empirical studies, the importance of different contingencies have emerged. These include the redundancy in the mapping of genotype to phenotype [28,29], i.e. how many genetic routes exist to replicate phenotypes? Limitations in this map are expected to upwardly bias reuse of the same genes or mutations, but redundancy can allow for the evolution of different genes in shared functional pathways. In addition, population structure dictates the sharing of adaptive variation among lineages by which selection may act on [30]. Finally, two lineages may experience an aspect of their environment in a similar way, but in a multidimensional sense environmental variation may limit genetic convergence through pleiotropic constraint [31]. This may result in the re-use of genes with minimal constraint and minimal effects on other aspects of fitness, as suggested for *MC1R* in pigmentation across vertebrates [32]. Alternatively, similarity of environments within multivariate space can predict genetic convergence [33–35], whereby consistencies in the multidimensional fitness landscape channel adaptation along conserved paths. These latter two limiting factors may also explain why genetic convergence can vary for the same traits in the

same species in global comparisons, for example in comparisons of Pacific-derived vs Atlantic-derived freshwater stickleback [35–37].

It is clear then to understand the complexity by which genetically convergent evolution might emerge requires study systems for which we already have abundant research on interactions between phenotype and environment. Here, we make use of a model of phenotypic convergence, the Trinidadian Guppy (*Poecilia reticulata*), to evaluate genetic convergence in the replicated adaptation of low-predation (LP) phenotypes from high-predation (HP) sources. For approaching 50 years, this system has provided valuable insights into phenotypic evolution in natural populations, including some of the first evidence of rapid phenotypic evolution in vertebrates across ecological, rather than evolutionary, timescales [38,39]. The guppy has since become a prominent model of phenotypic evolution in nature, but accompanying genomic work has only recently begun to emerge.

The topography of Northern Trinidad creates rivers punctuated by waterfalls, which restrict the movement of guppy predators upstream but not guppies themselves. This replicated downstream/HP and upstream/LP habitat has produced convergent HP-LP guppy phenotypes; LP guppies produce fewer, larger, offspring per brood [40,41], differ in shoaling behaviour [42,43], swimming performance [44] and predator evasion [45], and exhibit brighter sexual ornamentation [46]. Rearing second generation HP-LP guppies in a laboratory setting with controlled rearing conditions confirms that much of the life history differences have a genetic basis [47], and additional work has further demonstrated heritability for colour [48,49] and

89 behaviour [50]. Alongside studies of natural populations, the convergent and replicated nature
90 of these phenotypes has been established with experimental transplanting of HP populations
91 into previously uninhabited LP environments [38,51–53].
92
93 Here, we examine whole-genome sequencing of five replicated HP-LP population pairs across
94 the main drainages of Northern Trinidad. Previous work looking at HP-LP convergence in
95 natural HP-LP guppy populations using reduced representation RAD-sequencing found some
96 evidence of molecular convergence [54]. This study however only included three natural
97 populations pairs and inferences from RAD-sequencing can be limited by reliance on linkage
98 disequilibrium and an inability to pinpoint specific candidate genes. To comprehensively
99 explore genetic convergence in this system we first examine how genetic variation is distributed
100 across Northern Trinidad by quantifying population structure, between-river introgression, and
101 within-river demography. We then compare and contrast selection scans between HP-LP pairs
102 within each river to detect signals of convergent evolution. Finally, we examine a large
103 candidate haplotype to explain the mode and mechanisms by which convergence may have
104 occurred at this genomic region.
105

106 **RESULTS**

107 ***Population structure, admixture, and demographic history***

108 Prior to assessing genomic convergence, it is important to contextualise neutral processes such
109 as population structure, introgression and past demography in order to establish expectations
110 regarding how potentially adaptive genetic variation is distributed and shared among

111 populations; this informs on the most likely mode by which genetic convergence may occur in
112 this system.
113
114 Both principal component analysis (PCA) and fineSTRUCTURE [55] confirmed that each river's
115 HP-LP pair formed sister populations and structure between pairs (as river units) was well-
116 defined. Expectedly, the strongest population structure separated rivers by drainage, with PC1
117 (33.5%) separating rivers from the Caroni drainage (Guanapo [GHP,GLP], Aripo [APHP,APLP],
118 Tacarigua [TACHP,TACLP]]) from the Norhern and Oropouche drainages (Madamas [MADHP,
119 MADLP] and Oropouche [OHP, OLP] rivers, respectively) (Figure 1A,B). PC2 (19.8%) separated
120 out Caroni rivers, highlighting population structure within this drainage is stronger than
121 structure between Madamas and Oropouche, despite these rivers being in separate drainages.
122 Similarly, admixture proportions inferred by fineSTRUCTURE were lower on average between
123 rivers within the Caroni drainage than between Oropouche and Madamas (Figure 1C). This
124 structure within Caroni occurs despite longer branch lengths in Madamas and Oropouche
125 (Figure 1B) suggesting that the ancestral split between Caroni rivers and Northern/Oropouche
126 rivers is more ancient than the splits between Caroni rivers themselves (Figure 1C). We also
127 detected signatures of introgression into APHP from all Madamas and Oropouche populations,
128 categorised as elevated haplotype donor proportions of individuals from these rivers into APHP
129 recipients (Figure 1C).
130

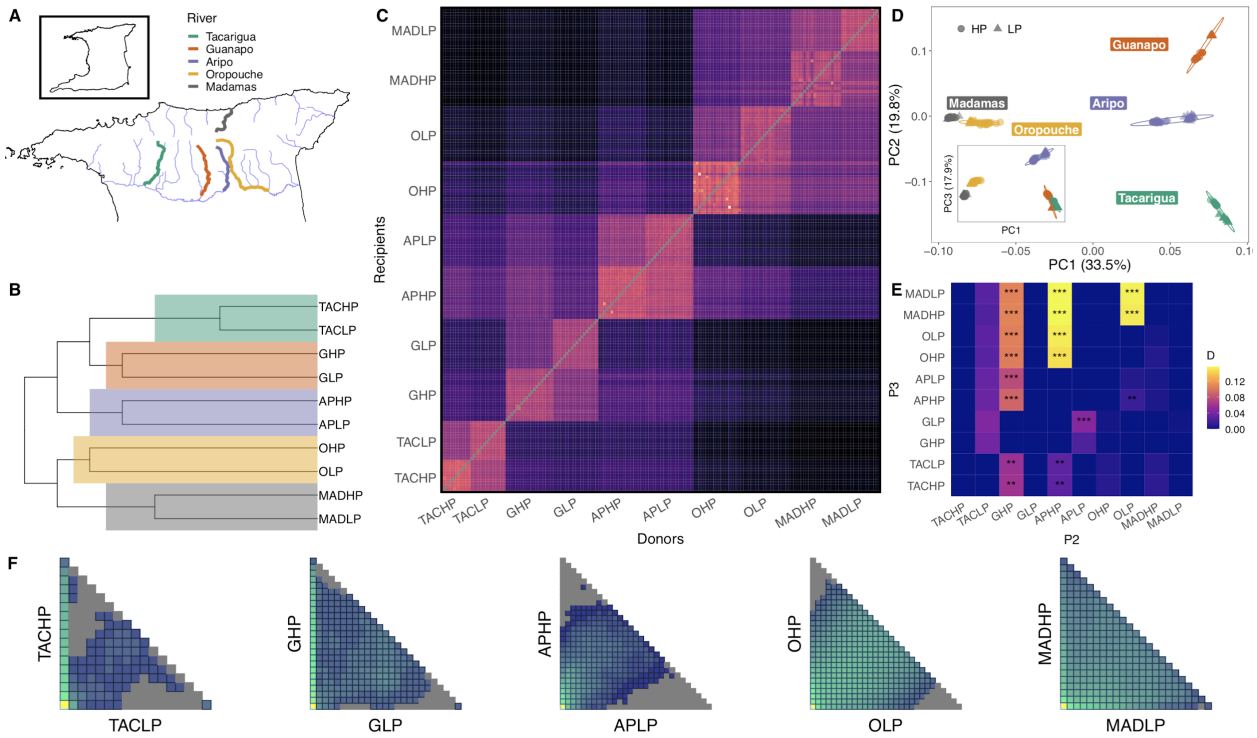

Figure 1: Sampling sites, population structure and admixture across the five rivers. Map (A) highlights sampled rivers from the three drainages in Northern Trinidad. Other major rivers are illustrated in light blue. Sampling rivers plotted alongside topography is available in Figure S1. Phylogenetic tree (B) based on chromosome painting and fineSTRUCTURE analysis, with river nodes highlighted. Heatmap (C) illustrates the proportion of painted recipient haplotypes based on donor haplotypes, used by fineSTRUCTURE to infer coancestry. PCA (D) with populations coloured according to river and shaped according to predation regime. PC3 and PC4 are presented in the insert. Heatmap (E) highlights introgression as pairwise, genome-wide D values between P2 and P3 populations. Populations within rivers were defined as P1 and P2, so all P2 and P3 pairings are between rivers. Two-dimensional site frequency spectra (2dsfs) for each river pair (F) highlighting the sharing of variants between LP and HP populations within each river. LP populations are on the x-axis and HP populations are on the y-axis. In each sfs, the frequency of sites in each population is illustrated from 0 to N, where N is the number of individuals in each population.

To quantify genome-wide introgression, we calculated D-statistics for trios with *Dsuite* (version 0.3; [56]). These were used primarily to infer introgression between populations in different rivers, therefore we focussed on trios where P1 and P2 were HP-LP pairs from the same river.

151 We recovered signals of significant genome-wide introgression in the form of D-statistics
152 (elevated sharing of derived sites between rather than within rivers) between APHP and both
153 populations in the Madamas and Oropouche rivers (D_{MADHP} = 0.156, p_{MADHP} = 0; D_{MADLP} = 0.156,
154 p_{MADLP} = 0; D_{OHP} = 0.147, p_{OHP} = 0; D_{OLP} = 0.152, p_{OLP} = 0) (Figure 1E). Comparing donor and
155 recipient haplotype proportions (Figure 1C) suggests that introgression has occurred at a
156 greater rate into, rather than out of, APHP. Further introgression was observed between
157 Madamas populations and OLP (D_{MADHP} = 0.154, p_{MADHP} = 0; D_{MADLP} = 0.152, p_{MADLP} = 0).
158 Haplotype proportions suggest directionality is greater into OLP. We also observed weak
159 introgression between both Tacarigua populations and APHP (D_{TACHP} = 0.030, p_{TACHP} = 6.12e-3;
160 D_{TACLP} = 0.030, p_{MADLP} = 6.94e-3), and more likely into APHP. Interestingly, we also detected
161 significant introgression between GLP and APLP (D = 0.05, p = 1.17e-7). Evidence of an extreme
162 bottleneck in GLP (see below) is the probable driver of elevated D statistics in comparisons with
163 GHP (Figure 1E), through a loss of within-river shared sites and excessive drift of *de novo*
164 variants in GLP. To detect introgression in spite of this between APLP and GLP suggests the
165 introgression we detected may be conservative.
166
167 To assess within river population demography (i.e. LP population bottlenecks, HP-LP migration),
168 we performed demographic modelling based on two-dimensional site frequency spectra (2dSFS)
169 using *fastsimcoal2 [57]*(Figure 1F; Table 1). All demographic models performed better with the
170 addition of migration, which in every case was higher downstream from LP to HP. For three rivers
171 (Aripo, Madamas, Tacarigua) a historic LP bottleneck was detected alongside stable current
172 population size. Guanapo was better supported by a model with no HP population growth, and

173 Oropouche by a model that suggested HP population growth. The particularly high estimates of
174 N_e in APHP agree with the above analyses of introgression into this population.
175

176 **Table 1**: Demographic parameters of each river, inferred by *fastsimcoal2*. Values in brackets
177 represent confidence intervals of 95% after bootstrapping 100 SFS.
178

Drainage	River	Mean HP-LP F_{ST}	HP N_e	LP N_e	HP > LP Migration	LP > HP Migration	Model
Caroni	Tacarigua	0.243	3,549 (2864-4493)	474 (347-612)	4.78e-5	1.55e-4	LP Bottleneck
Caroni	Guanapo	0.269	19,698 (19592-19698)	155 (135-183)	3.88e-6	8.34e-4	No population changes
Caroni	Aripo	0.072	43,354 (33767-59439)	6,122 (4588-9008)	2.10e-4	3.27e-4	LP Bottleneck
Oropouche	Oropouche	0.087	4,514 (4148-4910)	3,740 (3825-4411)	2.43e-4	1.21e-3	HP population growth
Northern	Madamas	0.171	1,121 (922-1355)	2,480 (2337-2743)	8.68e-5	4.88e-4	LP Bottleneck

179

180 Altogether, these analyses illustrate how genetic variation is segregated across the five rivers in
181 our dataset. Primarily, ancestral variation is dictated by geography, with populations defined
182 within rivers, then within drainages. Particularly strong population structuring is observed in
183 the Caroni drainage (Tacarigua, Guanapo and Aripo rivers), with limited evidence of
184 introgression having occurred among these rivers within drainage. In contrast, we detect
185 significant introgression across drainages, between the Madamas, Oropouche, and Aripo rivers,
186 demonstrating that these rivers are likely to share a greater proportion of genetic variation
187 than their drainage-structured phylogenetic history would otherwise suggest. These results are
188 consistent with the potential for introgression to occur between rivers through flooding, as the
189 mountainous regions between Tacarigua, Guanapo and Aripo rivers in the Western Caroni

190 drainage are higher and therefore would experience less connectivity during flooding events
191 (Figure S1).
192
193 Within rivers, we see evidence of population bottlenecks in LP populations, potentially limiting
194 the amount of available adaptive variation. This is particularly apparent in Tacarigua and
195 Guanapo, within which LP populations have particularly low N_e estimates, an excess of
196 monomorphic sites that are polymorphic in the HP founder, and only limited unique
197 polymorphic sites (Figure 1E). In other words, the variation within these LP populations is a
198 subset of that found in the corresponding HP. For all river pairs, our demographic modelling
199 agrees that migration upstream from HP to LP is weaker than LP to HP, compounding the
200 potential for limited variation upstream. Some HP-LP populations are better connected by
201 migration however, such as OHP and OLP, where many polymorphic sites are readily shared
202 between upstream and downstream.
203
204 ***Candidate HP-LP regions and assessing convergence***
205 To evaluate regions associated with HP-LP adaptation, we scanned the genome using several
206 approaches: XtX [58], a Bayesian analogue of F_{ST} that includes a simulated distribution under
207 neutrality; AFD, absolute allele frequency difference, which scales linearly from 0-1 between
208 undifferentiated and fully differentiated [59]; and XP-EHH (extended haplotype homozygosity)
209 [60], which compares homozygosity between phased haplotypes between populations. To
210 identify selected regions, we calculated each measure in non-overlapping 10kb windows within
211 each river between HP and LP sites. Putatively selected windows were identified if they were

212 detected as outliers by at least two approaches (see methods for outlier criteria for individual
213 tests; Figure S2). Using an intersect of all three may be over-conservative, for example, we
214 would miss instances where divergent selection within a river fixes alternate haplotypes and so
215 both HP and LP population have similarly low heterozygosity (i.e. no XP-EHH outlier but an
216 outlier in XtX and AFD).
217
218 Comparing the intersecting list of candidates of XtX, AFD and XP-EHH within each river revealed
219 little overlap among rivers, with only a single 10kb window overlapping in more than two rivers
220 (Figure 2A; for genome-wide plots see Figure S3-5). We then scanned the genome further with
221 100kb sliding windows (50kb increments) to assess potential clustering of outlier windows in
222 larger regions, but this approach similarly revealed little overlap among rivers. We then
223 explored whether outlier regions (10kb windows overlapping in >1 selection scans) were
224 enriched for genes in common biological pathways between rivers using one-to-one zebrafish
225 orthologues, which may suggest repeated pathway modification, albeit through different
226 genes. Using the outlier regions defined above, no pathway was significantly overrepresented
227 in any river. We did however notice cases in which the same pathways exhibited fold-
228 enrichments >1 in multiple rivers (Figure 2B), albeit non-significant within rivers in each case.
229 We used permutations to explore the likelihood of observing fold-enrichment >1 in our five
230 independently-derived outlier sets. This analysis identified that Cadherin-signalling pathway
231 genes were overrepresented across all five rivers relative to by-chance expectations (p = 0.013)
232 (Figure 2B). In total, 20 genes from the Cadherin-signalling pathway were recovered from all
233 five river outlier sets, with some overlap between them (Table S1). This analysis may be over-

conservative, due to analysing only guppy genes with one-to-one zebrafish orthologues. Other genes associated with cadherin-signalling were detected by our selection scans, including *Cadherin-1* and *B-Cadherin* in a differentiated region on chromosome 15 (~ 5 Mb) in Oropouche and Tacarigua, but these genes exhibited a many-to-many orthology with zebrafish genes so were omitted. We also examined pathways with fold-enrichment >1 in any four rivers, but these were not significant ($p > 0.05$) according to permutation tests (Figure 2B).

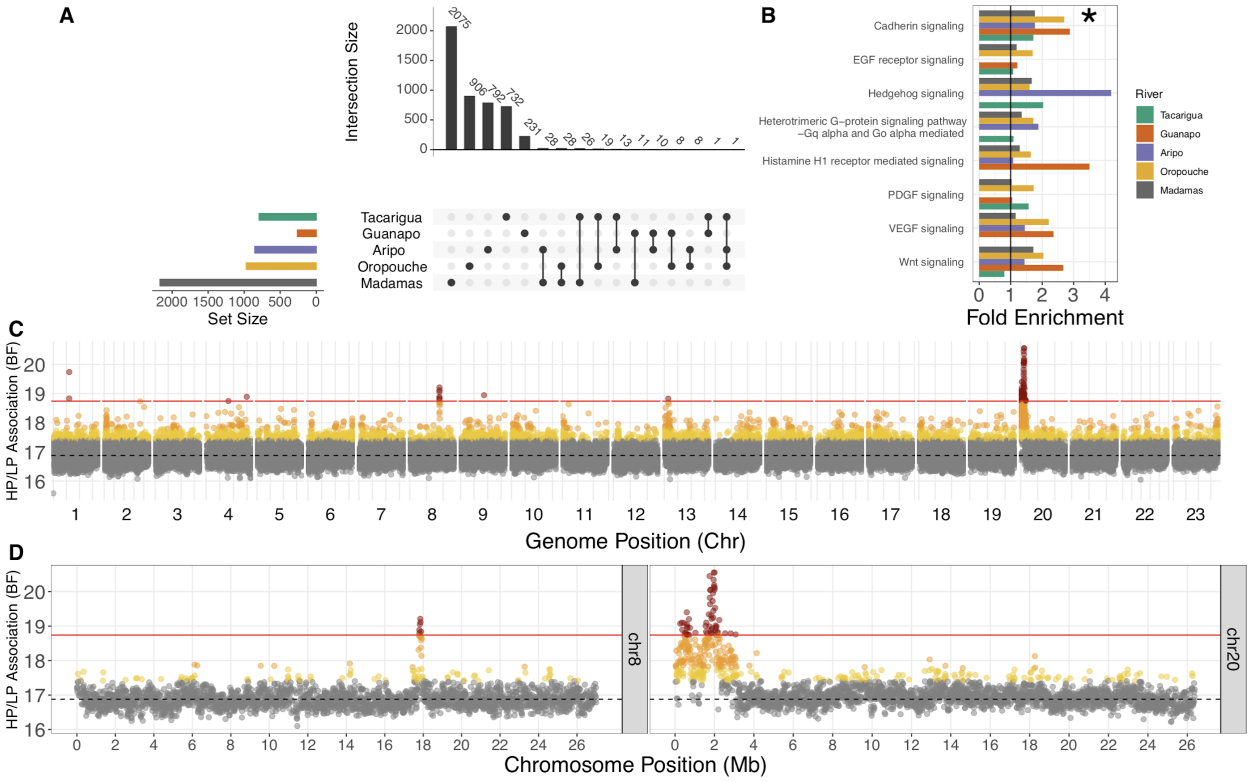

Figure 2: Selection scan results and evidence of convergence. Upset plot (**A**) of overlap among outlier sets (evidence from two of AFD, XtX, XP-EHH) highlighting no overlap beyond sets of three rivers. Fold enrichment of pathways (**B**) associated with zebrafish orthologs of genes in outlier regions within each river calculated from the Panther DB. Cadherin-signalling pathway was the only pathway with fold-enrichment >1 in all rivers. Other presented pathways had fold-enrichment >1 in four rivers. Genome-wide BayPass scan results (**C**) scanning 10kb windows for association with HP-LP classification. Points are coloured according to quantiles: 95% = yellow, 99% = orange, 99.9% = red. Dashed line represents the median BF, and the solid red line denotes 99.9% quantile cut-off. Peaks on chromosomes 8 and 20 are also highlighted **(D)**.

251

252 We next associated allele frequency changes with HP-LP status using BayPass' auxiliary
253 covariate model. This latter approach has the advantage of using all populations together in a
254 single analysis, whilst controlling for genetic covariance. Scans for regions associated with HP-LP
255 classification identified two major clusters of associated 10kb windows on chromosomes 8 and
256 20 (Figure 2C and 2D). In total, we highlighted 70 10kb windows corresponding to 24 annotated
257 genes (and a number of novel, uncharacterised genes) (Table S2). Intersecting these windows
258 with within-river candidate regions highlighted that most HP-LP associated candidates reflected
259 within-river selection scan outliers in one to three rivers (Table S3). Selection scans may
260 overlook some of our association outlier windows because differentiation at these loci may be
261 moderate, but rather we are detecting consistent allele frequency changes in the same
262 direction between HP-LP comparisons. Many of the associated windows mapped to a
263 previously unplaced scaffold in the genome (000094F), but we were able to place this at the
264 start of chromosome 20 along with some local rearrangements (Figure S6) using previously
265 published HiC data [61]. From here on and in Figure 2C-D, we refer to this new arrangement for
266 chromosome 20 and scaffold 000094F as chromosome 20.

267

268 The clusters on chromosomes 8 and 20 exhibited multiple 10kb windows above the 99.9%
269 quantile of window-averaged BF scores, suggesting larger regions associated with HP-LP
270 adaptation in multiple rivers (Figure 2D). In particular, the region at the start of chromosome 20
271 spanned several megabases with two distinct peaks. The larger of these peaks reflected the
272 strongest region of differentiation in the Aripo river (Figure S7) (which was minimally

differentiated genome-wide, Figure S5). We explored this candidate region further to evaluate: which rivers showed evidence of HP-LP differentiation within these regions; by what mode of convergence these regions had evolved under; and their gene content and probable candidates for HP-LP phenotypes.

Candidate Region on Chromosome 20

Visualisation of genotypes (Figure 3A) illustrated extended haplotype structures that were consistent with haplotypes spanning the entire chromosome 20 candidate region (Figure 2D). Interestingly, two of the three Caroni LP populations (GLP and TACLP) were fixed or nearly fixed for homozygous ALT haplotypes across the region (Figure 3A). We will refer to this entire region (~0-2.5 Mb) as the 'CL haplotype' (Caroni LP haplotype). The other haplotype we will refer to as the 'REF haplotype' due to its closer similarity to the reference genome. Moreover, a subset of the candidate region was nearly fixed in APLP (between black lines, between ~1.53 - 2.13 Mb, referred to as the CL-AP region Figure 3A). This CL-AP region corresponds to both the region of highest genome-wide divergence in Aripo (Figure S7), and the largest peak in our HP-LP association analysis (Figure 2D).

We then assessed whether ancestry of our candidate region (Figure 3B) deviated from the rest of chromosome 20 using a local PCA analysis. This approach is sensitive to inversions, changes in recombination and gene density [62], which may explain why such a large region appears as HP-LP associated. This approach confirmed that the associated region exhibits distinct local ancestry in relation to the rest of the chromosome in all five rivers (Figure 3B), albeit with some

295 idiosyncrasy. For example, MDS scaling along the major axis was broadly similar for GHP and
296 TACHP (LP populations were fixed and therefore showed minimal signal), with the entire region
297 segregated as a single block. In Aripo however, smaller blocks within the region were the major
298 drivers of local ancestry. Linkage analyses confirmed strong linkage across the several
299 megabases spanning the HP-LP associated region in most of the sampled populations (Figure
300 S8).
301
302 To understand the mode of convergence at the CL-AP region, we reconstructed the
303 phylogenetic history of the haplotype at this region. To start, we performed PCA analysis over
304 the CL-AP region, and found three clusters along a PC1 axis with large loading (PC1 = 57%,
305 Figure S9), consistent with individuals tending to either be homozygotes for either haplotype or
306 heterozygotes. We used these clusters to define homozygous individuals and explored the
307 phylogenetic history of these homozygote haplotypes following phasing. A maximum-likelihood
308 tree using RAxML-NG (version 0.9.0) illustrated that the CL haplotype at the CL-AP region is
309 phylogenetically distinct from the REF haplotype and separated by a long branch (Figure 3C).
310 This clustering of CL haplotypes and REF haplotypes contradicts the neutral expectation that
311 haplotypes should be predominantly structured within rivers. The clustering of Oropouche and
312 Madamas individuals with Caroni REF haplotypes was surprising, and in stark contrast to the
313 genome-wide phylogeny that clearly separates rivers by drainage (Figure 1B). We compared the
314 branch lengths along this tree among Caroni individuals with the CL haplotype at the CL-AP
315 region with non-Caroni individuals (Oropouche and Madamas) against branch lengths between
316 the same individuals from 50 100kb regions randomly selected from across the genome. This

317 analysis revealed that divergence between the REF and CL haplotype is in line with the modal
318 distance derived from the 50 random trees (Figure S10). This therefore suggests that the CL
319 haplotype may be as old as the split between Caroni and Northern/Oropouche drainage
320 lineages.
321
322 These patterns may be consistent with a large inversion, polymorphic in Caroni HP populations
323 but fixed in Caroni LP populations. Further structural variation (SV) or a recombination event
324 between the CL haplotype and the REF haplotype may then have released the CL-AP region
325 from the larger CL haplotype in Aripo only. We therefore explored the potential for inversions
326 and SVs with our aligned read data using smoove [63] (v0.2.5) and Breakdancer [64] (v1.4.5).
327 We did not find evidence for an inversion or an alternative SV spanning either the full CL
328 haplotype (in Guanapo or Tacarigua) or around the diverged CL-AP region in Aripo. Interestingly
329 however, this analysis of SVs did highlight that the strongest peak of HP-LP differentiation in the
330 Oropouche river (chromosome 15 at approximately 5Mb, Figure S11), was associated with a
331 detected 1.1 kb deletion within the *B-cadherin* gene, and exhibited high HP-LP F_{ST} (0.66).
332

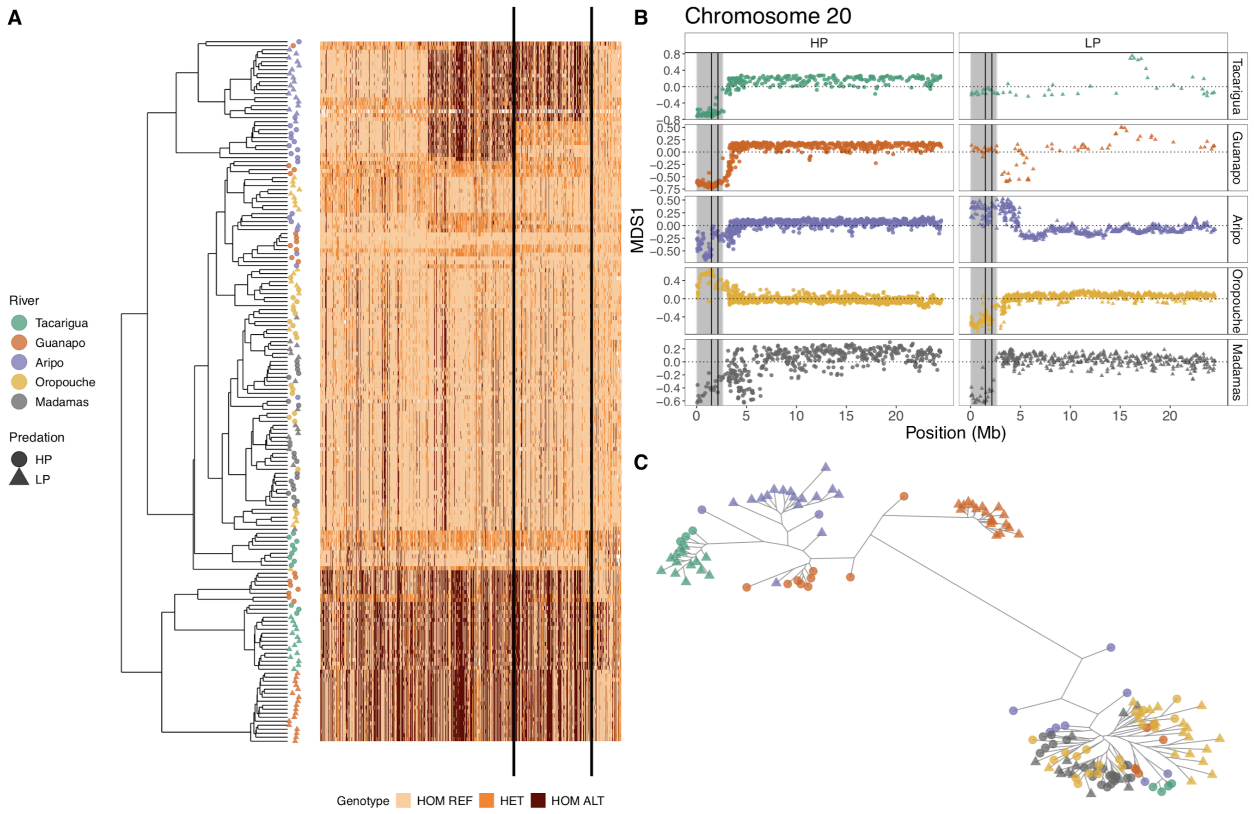

Figure 3: Evidence of divergence along the CL haplotype (ALT alleles, chr20:1-2633448); genotypes for each individual plotted according to hierarchical clustering (**A**). Solid black lines denote the CL-AP region, corresponding to the strongest peak of HP-LP association in the dataset. (**B)** The CL haplotype region (shaded grey) shows evidence of segregated local ancestry in comparison to the rest of chromosome 20, according to MDS scores derived from local PCA analysis. The CL-AP region is again shown between solid black lines. MDS1 = 0 is shown as a dotted line in each panel. A lack of signal on MDS1 for the CL region in Guanapo LP (GLP) and Tacarigua LP (TACLP) reflects that this region is fixed. (**C**) Unrooted maximum-likelihood tree of homozygous individuals (haplogroups) across the CL-AP region, highlighting a major phylogenetic branch separating Caroni LP individuals from both Caroni HP individuals (homozygous for the REF haplotype) and populations from outside the Caroni drainage.

It is particularly interesting that given the CL haplotype may be reasonably old, it has been broken down into smaller regions only in the Aripo river, whereas Tacarigua and Guanapo maintain the full haplotype. One unique attribute of Aripo is evidence of introgression from beyond its drainage. We therefore explored introgression signals (D-statistics) along

351 chromosome 20 between a trio of GH (P1), APHP (P2), and OH (P3) for individuals homozygous
352 for the REF haplotype (upper cluster, Figure 3C). We looked only at these individuals to remove
353 effects of haplotype heterozygosity in GH and APHP but not OH. This analysis strongly
354 suggested that the CL-AP region (and much of chromosome 20) in APHP has experienced
355 introgression with populations outside of the Caroni drainage (greater proportion of shared
356 sites between P2 and P3 compared with P1 and P2) (Figure S12).
357
358 Within the CL haplotype region there are 56 annotated genes (Table S4), several of which may
359 have important roles in HP-LP phenotypes. Due to the elevated differentiation observed across
360 the haplotype, it is difficult to pinpoint specific candidates. However, the breakdown of the
361 haplotype in Aripo at the CL-AP region, corresponding to our association peak, provides a
362 unique opportunity to narrow down candidate genes given it is the only part of the larger
363 candidate region that is differentiated in all Caroni HP-LP comparisons. Interestingly, analyses
364 of coverage across the CL-AP region uncovered repeatable low coverage in all Caroni LP
365 populations that corresponded with deletions of several kb (viewed in *igv*) in the LP populations
366 (Figure S13). Five of these deletions overlapped with the *plppr5* gene, including a deletion
367 subsuming the final exon of the gene (Figure S13B). This gene also spanned the HP-LP
368 associated windows with the highest association scores (Table S4). The adjacent *plppr4* gene
369 included the individual SNP (000094F_0:556282) with the highest HP-LP association score of all
370 SNPs in the genome (Figure S13A). This particular SNP was observed in the intron between the
371 second and third exons of *plppr4*.
372

373 In summary, this region presents a fascinating example of genetic convergence of an
374 ancestrally-inherited large haplotype among rivers in the Caroni drainage. As such, subsequent
375 genetic divergence of HP-LP adaptation is observed in non-Caroni rivers due to the presumed
376 loss of the CL haplotype in the lineage ancestral to non-Caroni rivers. Additionally, Aripo
377 exhibits a unique signature of stronger HP-LP differentiation at a subregion of the haplotype
378 due to a potentially more recent recombination event between the larger, diverged haplotypes
379 themselves. The CL-AP region exhibits a strong, whole-region signature of introgression with
380 rivers beyond the Caroni drainage (namely neighbouring Oropouche), suggesting that this
381 region of the genome has experienced between-river introgression that may have facilitated
382 haplotype breakdown of the larger CL haplotype.
383

384 **DISCUSSION**

385 Using a whole genome sequencing approach, we found a strong candidate haplotype for HP-LP
386 convergence within the Caroni drainage of Northern Trinidad (the only drainage where we have
387 multiple rivers sequenced), but we also found molecular convergence at specific loci is limited
388 among rivers from different drainages. Further, we find evidence that convergence at the level
389 of functional pathways among rivers may facilitate phenotypic convergence across all rivers.
390 Our convergent LP candidate region exhibited a strong signal of divergent selection between
391 HP-LP sites on chromosome 20. This region contains a large haplotype fixed or nearly fixed in LP
392 populations in all three Caroni rivers examined, and contained promising candidate genes for LP
393 phenotypes. This haplotype has largely been maintained as a tightly linked unit, with the
394 exception of Aripo, and likely evolved in these LP populations from shared variation common

395 within, and limited to, the Caroni HP sources. Our analysis of population structure, admixture,
396 and demographic histories across Northern Trinidad suggest that the reduced re-use of the
397 same alleles among drainages may be due to strict structuring of genetic variation between
398 some rivers and recurrent bottlenecks during the founding of LP populations from HP sources.
399 Combined, these processes limit shared ancestral genetic variation from which convergent
400 genetic adaptation may occur. This is not true for all rivers however, with some gene flow
401 taking place between rivers outside of the Caroni drainage and LP populations (APLP and OLP in
402 particular) with no evidence of limited genetic variation.
403
404 The candidate region on chromosome 20 was a clear outlier, with by far the strongest signal of
405 HP-LP association, and the majority of windows spanning the first 2.5 Mb of chromosome 20
406 were above the 99.9% BF cutoff. Interestingly however, most of these windows were only
407 outliers in Aripo for within-river selection scans. Further analysis found allele frequency
408 patterns of a large haplotype nearly fixed in all three LP Caroni drainage rivers (Aripo, Guanapo,
409 and Tacarigua). We termed this large haplotype the 'CL haplotype', and within this haplotype
410 the 'CL-AP region' as the strongest candidate for convergent HP-LP adaptation due to its
411 particularly strong HP-LP association peak and high within-river differentiation in Aripo. The
412 breakdown of the CL haplotype in Aripo, uniquely, may have been facilitated by introgression
413 from beyond the Caroni drainage. This observation stems from ABBA/BABA D-statistics
414 suggesting the CL-AP region in APHP has experienced introgression with OHP (Figure S12).
415

416 Recent empirical work has also shown the importance of large haplotype regions containing
417 many genes in convergent evolution. In *Littorina* these large divergent haplotypes are
418 maintained by inversions in crab vs wave ecotypes [65,66]. Similarly, sunflower species
419 repeatedly experience selection on large haplotypes [23], most, but not all, of which are
420 underwritten by inversions. This recent empirical evidence suggests a fundamental role of large
421 haplotype blocks in adaptation by bringing together and maintaining clusters of adaptive
422 alleles, although we cannot rule out genetic draft occurring around a single functional locus
423 within the CL haplotype. We did not detect evidence of inversions within this region, but given
424 that we detect deviations in local ancestry in all rivers (Figure 3B) relative to the rest of the
425 chromosome, and the acrocentric nature of guppy chromosomes [67], it is possible that
426 recombination is reduced over the CL haplotype due to proximity to the telomere. This
427 mechanism could maintain this haplotype in the absence of an inversion. We noted however
428 that, whilst the CL haplotype was fixed (at the CL-AP region) in Caroni LP populations, it was
429 polymorphic in all Caroni HP populations. Large haplotypes may bring together beneficial alleles
430 but they can generate constraint if different loci within the haplotype experience contrasting
431 selection. Through breakdown of the haplotype, potentially facilitated by introgression in Aripo,
432 release of genetic background constraints may have allowed for stronger HP-LP differentiation
433 at the CL-AP region uniquely in this river.
434
435 Within the CL-AP region we highlighted the *plppr5* and *plppr4* genes as strong candidates for
436 HP-LP adaptation. These genes correspond to the strongest signals of HP-LP association within
437 the CL-AP region, and in particular the *plppr5* allele on the CL haplotype is associated with an

438 exon-subsuming deletion (Figure S13B). There is limited functional evidence for these genes,
439 but evidence suggests a possible role in growth and body size. Transcriptome analysis has
440 shown that *PLPPR4* is among genes upregulated in slow-growth vs fast-growth Jinghai Yellow
441 Chicken chicks [68], and transgenic mice studies have demonstrated phenotypic effects of
442 *Plppr4* on body size and growth phenotypes [69]. In humans, *PLPPR4* expression is limited to
443 the brain, but *PLPPR5* expression occurs more broadly.
444
445 Across the CL haplotype region, HP populations were polymorphic, which is likely why we fail to
446 detect this region as within-river outliers in Guanapo and Tacarigua. Further, these rivers have
447 small LP populations and elevated signatures of genome-wide drift. That the CL haplotype
448 region is variable within HP populations suggests that there is selection on the CL haplotype in
449 LP populations but not against it in HP populations, or that downstream-biased migration is
450 strong enough to maintain the CL haplotype in downstream HP populations. At the CL-AP
451 region, we note that haplotypes derived from Oropouche and Madamas cluster with REF
452 haplotypes from Caroni (Figure 3C), despite genome-wide data suggesting the split between
453 Caroni and Northern/Oropouche drainage rivers is the deepest in our data (Figure 1B). Such
454 patterns can arise when diverged haplotypes are introgressed from more ancient lineages, or
455 even different species, as observed in flatfish [70], sunflowers [23], and *Heliconius* butterflies
456 [24]. We found, however, that branch lengths between the CL and REF haplotype clusters were
457 in keeping with internal branch lengths derived elsewhere in the genome (Figure S10),
458 suggesting it is unlikely that the CL haplotype has evolved elsewhere in an unknown lineage
459 before more recently introgressed into the Caroni drainage. This pattern suggests the CL

460 haplotype may have evolved prior to the splitting of Caroni, Northern, and Oropouche drainage
461 lineages, but was subsequently lost due to drift or selection outside of the Caroni drainage.
462
463 By using whole-genome data, we were able to explore in fine-detail how genetic variation is
464 structured and distributed across natural guppy populations across Northern Trinidad. Our
465 observations support previous work suggesting downstream-biased migration, strong drainage-
466 based structuring, and variable gene flow among rivers [71,72]. Using within-river demographic
467 analyses we also found downstream-biased migration in all rivers, but with variable rates, and
468 three LP populations experiencing bottlenecks; these bottlenecks likely represent historical
469 founding bottlenecks as opposed to recent crashes [71]. Such demographic processes, if strong
470 enough, can obscure signals of genetic convergence, or even produce false-positives by
471 manipulating the relative efficacy of selection and neutral processes across the genome [73].
472
473 An interesting observation from our introgression analyses was strong signals of introgression
474 in the Aripo HP population from the Oropouche and Madamas rivers. Aripo represents the most
475 easterly river within the Caroni drainage, whilst Oropouche/Quare is the most westerly river in
476 the Oropouche drainage (Figure 1A). Thus, admixture between these populations may be
477 possible, and indeed has been suggested elsewhere [52,72,74]; likely facilitated by flooding
478 during the wet season. We also found weaker, but significant, signals of introgression between
479 APLP and GLP which are upstream and adjacent. Introgression between upstream LP
480 populations has also been reported between the Paria and the Marianne rivers in the Northern
481 drainage [75], but is surprising given the more restrictive topography in the Caroni drainage

482 (Figure S1). The Aripo river may be particularly susceptible to contemporary human
483 translocations of guppies from across Trinidad, as it is heavily involved in active research
484 including experimental introductions.
485
486 These population structure results have important implications for the likelihood of observing
487 genetic convergence because they identify constraints on the sharing of ancestral genetic
488 variation through LP founding bottlenecks and limitations on adaptive variants being shared
489 among rivers [3]. Such structuring of genetic variation, typical of riverine populations, stands in
490 contrast to other prominent systems with abundant evidence of genomic convergence, such as
491 sticklebacks [76] and atlantic herring [77], where largely panmictic marine populations share
492 much adaptive variation. Standing genetic variation is a major contributor of adaptive variation
493 [78–80], and the sharing of this variation among lineages acts a significant contingency to
494 genetic convergence [81] in varied systems including fish [25,82] and insects [83].
495
496 Redundancy in the mapping of phenotype to genotype is expected for highly polygenic traits,
497 whereby many loci may be adapted to modify a phenotype, and in instances where phenotypes
498 are derived from complex functional pathways [28]. Indeed, convergence at the level of
499 pathways has been described for human pygmy phenotypes [15] and hymenopteran caste
500 systems [14]. In our selection scans, we found a greater proportion of genes associated with
501 cadherin-signalling than expected across five replicated datasets, suggesting this pathway may
502 be under selection at different genes in all rivers. Cadherin genes *cadherin-1* and *B-cadherin*
503 have previously been detected as under selection in experimentally transplanted LP

504 populations derived from GHP [54], however these specific genes, whilst also detected here,
505 were omitted from our pathway analysis due to many-to-one orthology with zebrafish genes.
506 Genes in this pathway have important roles in cell-cell adhesion, and are associated with tissue
507 morphogenesis and homeostasis by mediating interfacial tension and orchestrating the
508 mechanical coupling of contact cells [84]. Cadherin signalling pathways interact with the
509 signalling of various growth hormones and are involved in differential growth phenotypes. For
510 example, cadherin signalling genes were differentially expressed between transgenic and wild-
511 type coho salmon with divergent muscle fibre phenotypes that affect growth and the energetic
512 costs of maintenance [85]. Cadherin genes are also expressed during oogenesis in *Drosophila*
513 [86]. Assessing the functional roles of the cadherin signalling genes identified in our study
514 (Table S1) is beyond the scope of this work, but in identifying this pathway across rivers we
515 provide evidence for a potentially shared mechanism by which HP-LP phenotypes may similarly
516 evolve across Northern Trinidad.
517
518 It is also likely that contrasting demographic contexts within rivers, particularly migration
519 between HP-LP, can influence the genetic architecture of traits or the regions of the genome
520 where adaptive alleles reside. Theory predicts that with increasing sympatry, if multiple genetic
521 routes to a phenotype exist then traits should be underwritten by simpler genetic architectures
522 with fewer loci, each of larger effect [87,88]; such that favourable combinations of alleles are
523 less likely to be broken down by introgression. Empirical support from cichlid species pairs
524 suggests this is the case for male nuptial colour traits in sympatric vs allopatric pairs [89]. Given

525 demographic histories vary between our HP-LP populations (Table 1), these natural conditions
526 may moderate the selective benefits of different genetic routes to phenotypes.
527
528 In conclusion, we have investigated whether convergent HP-LP phenotypes that have evolved
529 repeatedly within rivers across Northern Trinidad are underpinned by convergent genetic
530 changes. We found convergence of genetic pathways not specific genes across drainages. This
531 is in keeping with recent work suggesting a predominant role of shared standing genetic
532 variation in driving convergent changes at the gene-level, a mechanism that is restricted in
533 natural guppy populations by limited between-river gene flow and recurrent founding
534 bottlenecks during LP colonisations. Within our drainage with multiple rivers sampled, we did
535 however find convergent evolution of a large haplotype region nearly fixed in Caroni LP
536 populations that is likely derived from shared ancestral variation between these populations.
537 These results provide a comprehensive, whole-genome perspective of genetic convergence in
538 the Trinidadian guppy, a model for phenotypic convergence.
539

540 **METHODS**

541 ***Sampling, Sequencing and SNP calling***
542 Individuals were sampled from naturally-occurring downstream HP and upstream LP
543 environments in rivers from each of Northern Trinidad's three drainages (Figure 1) between
544 2013 and 2017. Three of these rivers (Aripo, Guanapo, Tacarigua) share a drainage (Caroni),
545 whilst Oropouche (Oropouche) and Madamas (Northern) are found in separate drainages.
546 Numbers of individuals from each population were: TACHP = 12, TACLP = 14, GHP = 19, GLP =
547 18, APHP = 19, APLP = 19, OHP = 19, OLP = 20, MADHP = 20, MADLP = 16. Samples were stored
548 in 95% ethanol or RNeasy at 4° C prior to DNA extraction. Total genomic DNA was extracted
549 using the Qiagen DNeasy Blood and Tissue kit (QIAGEN; Heidelburg, Germany), following the
550 manufacturer's guidelines. DNA concentrations ≥ 35ng/µl were normalised to 500ng in 50µl and
551 were prepared as Low Input Transposase Enabled (LITE) DNA libraries at The Earlham Institute,

552 Norwich UK. LITE libraries were sequenced on an Illumina HiSeq4000 with a 150bp paired-end
553 metric and a target insert size of 300bp, and were pooled across several lanes so as to avoid
554 technical bias with a sequencing coverage target of ≥10x per sample. Data from the Guanapo
555 and Oropouche rivers has been previously published as part of Fraser et al. [61].
556
557 Paired-end reads were quality-controlled with fastQC (v0.11.7) and trimmed with trim_galore
558 (v0.4.5) before being aligned to the long-read, male guppy genome assembly [61] with bwa
559 mem (v0.7.17). Appropriate read groups were added followed by alignment indexing,
560 deduplication and merging to produce final bams. Merged, deduplicated alignments were
561 recalibrated using a truth-set of variants generated from high-coverage, PCR-free sequencing
562 data from 12 individuals [61]. GVCFs were produced using GATK's (v4.0.5.1) HaplotypeCaller
563 and consolidated to chromosome/scaffold intervals with GenomicsDBImport prior to
564 genotyping with GenotypeGVCFs.
565
566 SNPs were filtered on the basis of QD < 2.0, FS > 60.0, MQ < 40.0, HaplotypeScore > 13.0 and
567 MappingQualityRankSum < -12.5 according to GATK best practices. We retained only biallelic
568 sites with a depth ≥ 5. SNPs were also removed if missing in > 50% of individuals within a
569 population, if they were not present in all ten populations, and had a minor allele frequency <
570 0.05 (relative to all individuals). This produced a final dataset of 3,033,083 high-quality SNPs.
571
572 ***Population structure and introgression***
573 Principal Component Analysis was performed over all ten populations using a linkage-pruned (--
574 indep-pairwise 50 5 0.2) set of SNPs (N = 217,954) using plink (v2.00).
575
576 Prior to further estimates of population structure, chromosomes and scaffolds were phased
577 individually with beagle (v5.0; [90]), which performs imputation and phasing, and then phased
578 again using shapeit (v2.r904; [91]) making use of phase-informative reads (PIR). This method
579 has been effective elsewhere [92]. Phased chromosomes were re-merged into a single file for
580 analysis with fineSTRUCTURE (v4.0.1; [55]). FineSTRUCTURE first makes use of chromosome
581 painting before assessing admixture based on recombinant haplotype sharing among all
582 individuals. FineSTRUCTURE was run with a uniform recombination map and an inferred *c*-value
583 of 0.344942 with successful convergence.
584
585 We also estimated D-statistics for all 120 possible trios of the 10 populations using Dsuite [56].
586 Here, sequencing data from 10 *P. picta* individuals (5 males, 5 females) was aligned to the male
587 guppy genome using the protocol above to be used as an outgroup. bcftools consensus was
588 used to create a *P. picta* fasta file based on the final SNP variant calls and ancestral alleles were
589 inserted into the *P. reticulata* VCF files using *vcftools fill-aa*. We highlighted introgression
590 candidates as trios with significant D values (Bonferroni-corrected *p*-value < 0.05) between
591 populations from different rivers i.e. we retained trios for which P1 and P2 were assigned to the
592 same river by including the tree structure in Figure 1B to examine the possibility of
593 introgression between rivers. To examine further introgression along chromosomes, we
594 calculated D-values in non-overlapping windows of 100 SNPs.
595

596 ***Demographic inference***
597 We explicitly modelled the demographic history of each HP-LP population pair using
598 *fastsimcoal2* [57]. Fastsimcoal2 uses a continuous-time sequential Markovian coalescent
599 approximation to estimate demographic parameters from the site frequency spectrum (SFS). As
600 the SFS is sensitive to missing data, a --max-missing filter of 80% was applied to each population
601 vcf containing both monomorphic and polymorphic variants, and to remove LD, the vcf was
602 thinned at an interval of 20kb using *vcftools* [93]. For each HP-LP population pair, we generated
603 a folded two-dimensional frequency spectrum (2dSFS) using the minor allele frequency, which
604 were generated via projections that maximised the number of segregating sites using easySFS
605 (https://github.com/isaacovercast/easySFS).
606
607 Five demographic models were used to explore the demographic history of the population
608 pairs, all of which contained a uniform distribution divergence of 1 to 6e7 and log uniform
609 distribution N_E of 1 to 50000: Model A) HP-LP split with no population growth; Model B) HP-LP
610 split with no population growth and a post-founding bottleneck in the LP population; Model C)
611 HP-LP split with historical population growth in HP; Model D) HP-LP split with historical
612 population growth in HP and a post-founding bottleneck in the LP population; Model E) HP-LP
613 split with bottlenecks in both LP and HP populations. All five models were also run with the
614 inclusion of a migration matrix between LP and HP with a log uniform distribution of 1e-8 to 1e-
615 2. Fastsimcoal2 was used to estimate the expected joint SFS generated from 100 independent
616 runs, each consisting of 200,000 simulations per estimate (-n), generated by 100 ECM cycles (-
617 L). Model choice was assessed by computing the log likelihood ratio distributions based on
618 simulating 100 expected SFS from the run with the lowest delta (smallest difference between
619 MaxEstLhood and MaxObsLhood) as per Bagley et al. [94]. The most likely model was selected
620 for each population pair and the run with the lowest delta likelihood was used as input for
621 bootstrapping by simulating 100 SFS. We report the median and 95% confidence intervals for
622 N_E and probabilities of migration as provided by bootstrapping.
623
624 ***Scans for selection***
625 We used three approaches to scan the genome for signatures of selection between HP-LP
626 populations. We first estimated XtX (a Bayesian approximation of F_{ST}) within each river using
627 Baypass [58], which has the advantage of including a genetic covariance matrix to account for
628 some demographic variation. Genetic covariance matrices were estimated using LD-pruned
629 (plink --indep-pairwise 50 5 0.2) VCFs for each river, and averaged over 10 independent runs.
630 We determined a significance threshold within each river by simulating neutral XtX of a POD
631 sample of 10,000 SNPs with the *simulate.baypass()* function in R. We then marked 10kb
632 windows as outliers if their mean XtX value exceeded the 0.95 quantile of the neutrally
633 simulated distribution. Secondly, absolute allele frequency differences (AFD) were estimated by
634 taking allele counts from each population (vcftools --counts2) and estimating frequency
635 changes per SNP. To convert per SNP values to 10kb non-overlapping windows we removed
636 invariants within each river, calculated the median AFD, and filtered windows that contained
637 fewer than 6 SNPs. We marked outliers as windows above the upper 0.95 quantile, or with an
638 AFD > 0.5 if this quantile was > 0.5. The linear association with AFD and differentiation,
639 compared to the non-linear equivalent for F_{ST} makes this comparable measure of allele

640 frequency change more interpretable [59]. A cutoff of AFD = 0.5 therefore represents the
641 minimum by which to observe a change in the major allele between HP and LP. Finally, we
642 estimated the extended haplotype homozygosity score XP-EHH between each river with selscan
643 (v1.2.0a; [95]) and normalised in windows of 10kb. We limited this analysis to chromosomes
644 and scaffolds > 1 Mb in size, due to extreme estimates on smaller scaffolds distorting
645 normalisation. Outliers were marked as those with normalised XP-EHH > 2.
646
647 Enrichment analyses were performed by extracting one-to-one zebrafish orthologues for guppy
648 genes in outlier windows using Ensembl's BioMart (release 101; [96]). Orthologues were then
649 assessed for enrichment within rivers by comparing outlier genes against a background set of
650 all genome-wide guppy-zebrafish one-to-one orthologues using PantherDB [97]. Results from
651 all rivers were then compared in a single analysis to assess the above-expected enrichment of
652 functional groups across the entire dataset. We performed random permutations (N=10,000) to
653 draw equivalently sized within-river sets of outliers with weightings based on the number of
654 genes within each functional pathway group within the guppy-zebrafish orthologue background
655 gene set. Based on permuted random outlier sets, we then assessed the by-chance likelihood of
656 observing within-river enrichment >1 for all five or any four rivers for each of the functional
657 groups where this had been observed (groups plotted in Figure 2B).
658
659 For associated allele frequency changes with HP-LP classification, we also applied BayPass's
660 auxillary covariate model, which associates allele frequencies with an environmental covariate
661 whilst accounting for spatial dependency among SNPs with an Ising prior (-isingbeta 1.0). We
662 used a genetic covariance matrix including all 10 populations estimated as above. We split our
663 SNP data into 16 subsets, allocating alternate SNPs to each subset such that all subsets included
664 SNPs from all regions of the genome, and merged outputs as recommended in the manual. We
665 averaged per SNP BayesFactor scores within 10kb and marked as outliers those above the 0.999
666 quantile. We also explored alternative windowing strategies here, such as marking outlier SNPs
667 above the 0.999 quantile and determining window significance as windows with significantly
668 more outlier SNPs than a binomial (99.9%) expectation, however this made a minimal impact
669 on which windows were deemed outliers.
670
671 ***Characterisation of structural variants***
672 To assess whether candidate regions may contain structural variants, particularly inversions, we
673 first used local PCA analysis within each population for each chromosome with the R package
674 *lostruct* (v0.0.0.9) [62]. This method explores phylogenetic relationships between individuals
675 using windows of N SNPs along a chromosome, and then uses multidimensional scaling to
676 visualise chromosomal regions that deviate from the chromosomal consensus among
677 individuals. We filtered each population's chromosome for invariants, prior to running local PCA
678 in windows of 100 SNPs. For each run, we retained the first two eigenvectors (k=2) and
679 computed over the first two PCs (npc=2).
680
681 We used two methods to call structural variants from our final bam files: smoove (v0.2.5; [63])
682 (a framework utilising lumpy [98]) and Breakdancer (v1.4.5; [64]). For both methods we called
683 structural variants across all HP and LP individuals within a river. For smoove variants, we

684 excluded repetitive regions of the genome prior to variant calling, and filtered the subsequent
685 VCF for SVs marked as imprecise; <1kb in size; less read pair support (SU) than the per-river
686 median; without both paired-end and split-read support (PE | SR == 0). Breakdancer was run
687 per river, per chromosome, with results filtered for SVs <1kb in size; less support than per river,
688 per chromosome median support; quality < 99. We calculated F_{ST} using smoove VCFs within
689 each river to explore structural variants that may have diverged within rivers. To validate SVs of
690 interest, we plotted all bam files within a river using samplot [99] and visualised regions in *igv*.
691
692 ***Phylogenetic relationships of haplotypes***
693 To examine phylogenetic relationships of the CL haplotype, we calculated maximum likelihood
694 trees among homozygote haplogroups using RAxML-NG (v0.9.0; [100]). We limited this analysis
695 to the CL-AP region, which was subsumed within the larger CL haplotype in Guanapo and
696 Tacarigua and included the strongest region of HP-LP association (CL-AP region). Haplogroups
697 were defined on the basis of PC1 clusters (Figure S9). We retained a random haplotype from
698 homozygote individuals from all populations and constructed a tree using the GTR + Gamma
699 model with bootstrap support added (500 trees) with a cut-off of 3%.
700
701 To compare against other regions of genome, we randomly sampled 50 regions of the genome
702 of 100kb for the same individuals, repeated the above method for tree calculations, and
703 estimated branch lengths between individuals Caroni drainage individuals from the CL
704 haplogroup and Oropouche/Madamas individuals from the REF haplogroup.
705

706 ## AUTHOR CONTRIBUTIONS

707
708 JRW wrote the manuscript and performed all statistical and genomic analyses with the exception
709 of demographic modelling, which was done by JRP and MJvdZ. JRP, MJvdZ and PP were involved
710 in wet lab work including DNA extraction and library preps. DW procured grants for sampling.
711 BAF conceived and supervised the project, wrote and edited parts of the manuscript, undertook
712 sampling in Trinidad and was responsible for all other funding.
713

714 ## ACKNOWLEDGEMENTS

715
716 Kim Hughes and Mitchel Daniel for *Poecilia picta* specimens. David Reznick for support in
717 sampling logistics. HPC infrastructure support was provided by The University of Exeter's High-
718 Performance Computing (HPC) facility (ISCA). DNA sequencing was performed by University of
719 Exeter Sequencing Service (ESS). Batch submission scripts for *fastsimcoal2* analyses were kindly
720 provided by Vitor Sousa.
721

722 ## FUNDING

723
724 JRW, PJP, and BAF are funded by the EU (GUPPYCon 758382). DW is funded by the Max Planck
725 Society. This project utilised equipment funded by the Wellcome Trust Institutional Strategic

Support Fund (WT097835MF), Wellcome Trust Multi User Equipment Award (WT101650MA) and BBSRC LOLA award (BB/K003240/1).

DATA ACCESSIBILITY (To be updated upon acceptance)

Population genomics data are available on ENA: Study: XXX
Scripts used to analyse data are available from an archived github repository: Zenodo DOI: XXX

COMPETING INTERESTS

The authors declare no competing interests.

REFERENCES

1. Arendt J, Reznick D. Convergence and parallelism reconsidered: what have we learned about the genetics of adaptation? Trends Ecol Evol. 2008;23: 26–32.

2. Stuart YE. Divergent Uses of “Parallel Evolution” during the History of The American Naturalist. Am Nat. 2019;193: 11–19.

3. Stern DL. The genetic causes of convergent evolution. Nat Rev Genet. 2013;14: 751–764.

4. Fraser BA, Whiting JR. What can be learned by scanning the genome for molecular convergence in wild populations? Ann N Y Acad Sci. 2019. doi:10.1111/nyas.14177

5. Lee KM, Coop G. Population genomics perspectives on convergent adaptation. Philos Trans R Soc Lond B Biol Sci. 2019;374: 20180236.

6. Losos JB. Convergence, adaptation, and constraint. Evolution. 2011;65: 1827–1840.

7. Horn RL, Marques AJD, Manseau M, Golding B, Klütsch CFC, Abraham K, et al. Parallel evolution of site-specific changes in divergent caribou lineages. Ecol Evol. 2018;8: 6053–6064.

8. Colosimo PF. Widespread Parallel Evolution in Sticklebacks by Repeated Fixation of Ectodysplasin Alleles. Science. 2005;307: 1928–1933.

9. Foote AD, Liu Y, Thomas GWC, Vinař T, Alföldi J, Deng J, et al. Convergent evolution of the genomes of marine mammals. Nat Genet. 2015;47: 272–275.

10. Xie KT, Wang G, Thompson AC, Wucherpfennig JI, Reimchen TE, MacColl ADC, et al. DNA fragility in the parallel evolution of pelvic reduction in stickleback fish. Science. 2019;363: 81–84.

760 11. Protas ME, Hersey C, Kochanek D, Zhou Y, Wilkens H, Jeffery WR, et al. Genetic analysis of
761 cavefish reveals molecular convergence in the evolution of albinism. Nat Genet. 2006;38:
762 107–111.

763 12. Tenaillon O, Rodríguez-Verdugo A, Gaut RL, McDonald P, Bennett AF, Long AD, et al. The
764 molecular diversity of adaptive convergence. Science. 2012;335: 457–461.

765 13. Foll M, Gaggiotti OE, Daub JT, Vatsiou A, Excoffier L. Widespread signals of convergent
766 adaptation to high altitude in Asia and america. Am J Hum Genet. 2014;95: 394–407.

767 14. Berens AJ, Hunt JH, Toth AL. Comparative transcriptomics of convergent evolution:
768 different genes but conserved pathways underlie caste phenotypes across lineages of
769 eusocial insects. Mol Biol Evol. 2015;32: 690–703.

770 15. Bergey CM, Lopez M, Harrison GF, Patin E, Cohen JA, Quintana-Murci L, et al. Polygenic
771 adaptation and convergent evolution on growth and cardiac genetic pathways in African
772 and Asian rainforest hunter-gatherers. Proc Natl Acad Sci U S A. 2018;115: E11256–
773 E11263.

774 16. Wang L, Josephs EB, Lee KM, Roberts LM, Rellán-Álvarez R, Ross-Ibarra J, et al. Molecular
775 Parallelism Underlies Convergent Highland Adaptation of Maize Landraces. 2020. p.
776 2020.07.31.227629. doi:10.1101/2020.07.31.227629

777 17. Dobler S, Dalla S, Wagschal V, Agrawal AA. Community-wide convergent evolution in insect
778 adaptation to toxic cardenolides by substitutions in the Na,K-ATPase. Proc Natl Acad Sci U
779 S A. 2012;109: 13040–13045.

780 18. Storz Jay F., Natarajan Chandrasekhar, Signore Anthony V., Witt Christopher C.,
781 McCandlish David M., Stoltzfus Arlin. The role of mutation bias in adaptive molecular
782 evolution: insights from convergent changes in protein function. Philos Trans R Soc Lond B
783 Biol Sci. 2019;374: 20180238.

784 19. Nelson TC, Cresko WA. Ancient genomic variation underlies repeated ecological adaptation
785 in young stickleback populations. Evol Lett. 2018;2: 9–21.

786 20. Bohutínská M, Vlček J, Yair S, Laenen B, Konečná V, Fracassetti M, et al. Genomic basis of
787 parallel adaptation varies with divergence in Arabidopsis and its relatives. 2020. p.
788 2020.03.24.005397. doi:10.1101/2020.03.24.005397

789 21. Giska I, Farelo L, Pimenta J, Seixas FA, Ferreira MS, Marques JP, et al. Introgression drives
790 repeated evolution of winter coat color polymorphism in hares. Proc Natl Acad Sci U S A.
791 2019. doi:10.1073/pnas.1910471116

792 22. Le Moan A, Gagnaire P-A, Bonhomme F. Parallel genetic divergence among coastal-marine
793 ecotype pairs of European anchovy explained by differential introgression after secondary
794 contact. Mol Ecol. 2016;25: 3187–3202.

795 23. Todesco M, Owens GL, Bercovich N, Légaré J-S, Soudi S, Burge DO, et al. Massive
796 haplotypes underlie ecotypic differentiation in sunflowers. Nature. 2020;584: 602–607.

797 24. Edelman NB, Frandsen PB, Miyagi M, Clavijo B, Davey J, Dikow RB, et al. Genomic
798 architecture and introgression shape a butterfly radiation. Science. 2019;366: 594–599.

799 25. Bassham S, Catchen J, Lescak E, von Hippel FA, Cresko WA. Repeated Selection of
800 Alternatively Adapted Haplotypes Creates Sweeping Genomic Remodeling in Stickleback.
801 Genetics. 2018;209: 921–939.

802 26. Pease JB, Haak DC, Hahn MW, Moyle LC. Phylogenomics Reveals Three Sources of Adaptive
803 Variation during a Rapid Radiation. PLoS Biol. 2016;14: e1002379.

804 27. Kreiner JM, Giacomini DA, Bemm F, Waithaka B, Regalado J, Lanz C, et al. Multiple modes
805 of convergent adaptation in the spread of glyphosate-resistant Amaranthus tuberculatus.
806 Proc Natl Acad Sci U S A. 2019. doi:10.1073/pnas.1900870116

807 28. Yeaman S, Gerstein AC, Hodgins KA, Whitlock MC. Quantifying how constraints limit the
808 diversity of viable routes to adaptation. PLoS Genet. 2018;14: e1007717.

809 29. Láruson ÁJ, Yeaman S, Lotterhos KE. The Importance of Genetic Redundancy in Evolution.
810 Trends Ecol Evol. 2020;35: 809–822.

811 30. Blount ZD, Lenski RE, Losos JB. Contingency and determinism in evolution: Replaying life's
812 tape. Science. 2018;362. doi:10.1126/science.aam5979

813 31. Storz JF. Causes of molecular convergence and parallelism in protein evolution. Nat Rev
814 Genet. 2016;17: 239–250.

815 32. Manceau M, Domingues VS, Linnen CR, Rosenblum EB, Hoekstra HE. Convergence in
816 pigmentation at multiple levels: mutations, genes and function. Philos Trans R Soc Lond B
817 Biol Sci. 2010;365: 2439–2450.

818 33. Stuart YE, Veen T, Weber JN, Hanson D, Ravinet M, Lohman BK, et al. Contrasting effects of
819 environment and genetics generate a continuum of parallel evolution. Nat Ecol Evol.
820 2017;1: 158.

821 34. De Lisle SP, Bolnick DI. A multivariate view of parallel evolution. Evolution. 2020;74: 1466–
822 1481.

823 35. Magalhaes IS, Whiting JR, D'Agostino D, Hohenlohe PA, Mahmud M, Bell MA, et al.
824 Intercontinental genomic parallelism in multiple adaptive radiations. bioRxiv. 2019. p.
825 856344. doi:10.1101/856344

826 36. Paccard A, Hanson D, Stuart YE, von Hippel FA, Kalbe M, Klepaker T, et al. Repeatability of
827 Adaptive Radiation Depends on Spatial Scale: Regional Versus Global Replicates of

828 Stickleback in Lake Versus Stream Habitats. J Hered. 2019. doi:10.1093/jhered/esz056

829 37. Fang B, Kemppainen P, Momigliano P, Feng X, Merilä J. On the causes of geographically
830 heterogeneous parallel evolution in sticklebacks. Nat Ecol Evol. 2020;4: 1105–1115.

831 38. Endler JA. Natural Selection on Color Patterns in Poecilia reticulata. Evolution. 1980;34:
832 76–91.

833 39. Reznick DN, Shaw FH, Rodd FH, Shaw RG. Evaluation of the Rate of Evolution in Natural
834 Populations of Guppies. Science. 1997;275: 1934–1937.

835 40. Reznick D, Endler JA. The Impact of Predation on Life History Evolution in Trinidadian
836 Guppies (Poecilia reticulata). Evolution. 1982;36: 160–177.

837 41. Reznick DN, Rodd FH, Cardenas M. Life-History Evolution in Guppies (Poecilia reticulata:
838 Poeciliidae). IV. Parallelism in Life-History Phenotypes. Am Nat. 1996;147: 319–338.

839 42. Seghers BH, Magurran AE. Population differences in the schooling behaviour of the
840 Trinidad guppy, Poecilia reticulata: adaptation or constraint? Can J Zool. 1995;73: 1100–
841 1105.

842 43. Seghers BH. SCHOOLING BEHAVIOR IN THE GUPPY (POECILIA RETICULATA): AN
843 EVOLUTIONARY RESPONSE TO PREDATION. Evolution. 1974;28: 486–489.

844 44. Ghalambor CK, Reznick DN, Walker JA. Constraints on adaptive evolution: the functional
845 trade-off between reproduction and fast-start swimming performance in the Trinidadian
846 guppy (Poecilia reticulata). Am Nat. 2004;164: 38–50.

847 45. O'Steen S, Cullum AJ, Bennett AF. Rapid evolution of escape ability in Trinidadian guppies
848 (Poecilia reticulata). Evolution. 2002;56: 776–784.

849 46. Endler JA. A predator's view of animal color patterns. Evolutionary biology. Springer; 1978.
850 pp. 319–364.

851 47. Reznick D. The impact of predation on life history evolution in Trinidadian guppies: genetic
852 basis of observed life history patterns. Evolution. 1982;36: 1236–1250.

853 48. Hughes KA, Rodd FH, Reznick DN. Genetic and environmental effects on secondary sex
854 traits in guppies (Poecilia reticulata). J Evol Biol. 2005;18: 35–45.

855 49. Tripathi N, Hoffmann M, Willing E-M, Lanz C, Weigel D, Dreyer C. Genetic linkage map of
856 the guppy, Poecilia reticulata, and quantitative trait loci analysis of male size and colour
857 variation. Proc Biol Sci. 2009;276: 2195–2208.

858 50. Huizinga M, Ghalambor CK, Reznick DN. The genetic and environmental basis of adaptive
859 differences in shoaling behaviour among populations of Trinidadian guppies, Poecilia

860 reticulata. J Evol Biol. 2009;22: 1860–1866.

861 51. Kemp DJ, Reznick DN, Grether GF, Endler JA. Predicting the direction of ornament
862 evolution in Trinidadian guppies (Poecilia reticulata). Proceedings of the Royal Society B:
863 Biological Sciences. 2009;276: 4335–4343.

864 52. Fitzpatrick SW, Gerberich JC, Kronenberger JA, Angeloni LM, Funk WC. Locally adapted
865 traits maintained in the face of high gene flow. Ecol Lett. 2015;18: 37–47.

866 53. Reznick DN, Bassar RD, Handelsman CA, Ghalambor CK, Arendt J, Coulson T, et al. Eco-
867 Evolutionary Feedbacks Predict the Time Course of Rapid Life-History Evolution. Am Nat.
868 2019;194: 671–692.

869 54. Fraser BA, Künstner A, Reznick DN, Dreyer C, Weigel D. Population genomics of natural and
870 experimental populations of guppies (Poecilia reticulata). Mol Ecol. 2015;24: 389–408.

871 55. Lawson DJ, Hellenthal G, Myers S, Falush D. Inference of population structure using dense
872 haplotype data. PLoS Genet. 2012;8: e1002453.

873 56. Malinsky M, Matschiner M, Svardal H. Dsuite - fast D-statistics and related admixture
874 evidence from VCF files. Mol Ecol Resour. 2020. doi:10.1111/1755-0998.13265

875 57. Excoffier L, Dupanloup I, Huerta-Sánchez E, Sousa VC, Foll M. Robust demographic
876 inference from genomic and SNP data. PLoS Genet. 2013;9: e1003905.

877 58. Gautier M. Genome-Wide Scan for Adaptive Divergence and Association with Population-
878 Specific Covariates. Genetics. 2015;201: 1555–1579.

879 59. Berner D. Allele Frequency Difference AFD¯An Intuitive Alternative to FST for Quantifying
880 Genetic Population Differentiation. Genes . 2019;10. doi:10.3390/genes10040308

881 60. Sabeti PC, Varilly P, Fry B, Lohmueller J, Hostetter E, Cotsapas C, et al. Genome-wide
882 detection and characterization of positive selection in human populations. Nature.
883 2007;449: 913–918.

884 61. Fraser BA, Whiting JR, Paris JR, Weadick CJ, Parsons PJ, Charlesworth D, et al. Improved
885 reference genome uncovers novel sex-linked regions in the guppy (Poecilia reticulata).
886 Genome Biol Evol. 2020. doi:10.1093/gbe/evaa187

887 62. Li H, Ralph P. Local PCA Shows How the Effect of Population Structure Differs Along the
888 Genome. Genetics. 2019;211: 289–304.

889 63. Pedersen B. smoove: structural variant calling and genotyping with existing tools, but,
890 smoothly. Github; 2020. Available: https://github.com/brentp/smoove

891 64. Fan X, Abbott TE, Larson D, Chen K. BreakDancer: Identification of Genomic Structural

892 Variation from Paired-End Read Mapping. Curr Protoc Bioinformatics. 2014;45: 15.6.1–11.

893 65. Faria R, Chaube P, Morales HE, Larsson T, Lemmon AR, Lemmon EM, et al. Multiple
894 chromosomal rearrangements in a hybrid zone between Littorina saxatilis ecotypes. Mol
895 Ecol. 2018. doi:10.1111/mec.14972

896 66. Morales HE, Faria R, Johannesson K, Larsson T, Panova M, Westram AM, et al. Genomic
897 architecture of parallel ecological divergence: Beyond a single environmental contrast.
898 Science Advances. 2019;5: eaav9963.

899 67. Charlesworth D, Zhang Y, Bergero R, Graham C, Gardner J, Yong L. Using GC content to
900 compare recombination patterns on the sex chromosomes and autosomes of the guppy,
901 Poecilia reticulata, and its close outgroup species. Mol Biol Evol. 2020 [cited 11 Sep 2020].
902 doi:10.1093/molbev/msaa187

903 68. Chen F, Wu P, Shen M, He M, Chen L, Qiu C, et al. Transcriptome Analysis of Differentially
904 Expressed Genes Related to the Growth and Development of the Jinghai Yellow Chicken.
905 Genes . 2019;10. doi:10.3390/genes10070539

906 69. Dickinson ME, Flenniken AM, Ji X, Teboul L, Wong MD, White JK, et al. High-throughput
907 discovery of novel developmental phenotypes. Nature. 2016;537: 508–514.

908 70. Le Moan A, Bekkevold D, Hemmer-Hansen J. Evolution at two time-frames: ancient and
909 common origin of two structural variants involved in local adaptation of the European
910 plaice (Pleuronectes platessa). bioRxiv. 2020. p. 662577. doi:10.1101/662577

911 71. Barson NJ, Cable J, Van Oosterhout C. Population genetic analysis of microsatellite
912 variation of guppies (Poecilia reticulata) in Trinidad and Tobago: Evidence for a dynamic
913 source-sink metapopulation structure, founder events and population bottlenecks. J Evol
914 Biol. 2009;22: 485–497.

915 72. Willing E-M, Bentzen P, van Oosterhout C, Hoffmann M, Cable J, Breden F, et al. Genome-
916 wide single nucleotide polymorphisms reveal population history and adaptive divergence
917 in wild guppies. Mol Ecol. 2010;19: 968–984.

918 73. Whiting JR, Fraser BA. Contingent Convergence: The Ability To Detect Convergent Genomic
919 Evolution Is Dependent on Population Size and Migration. G3 . 2019.
920 doi:10.1534/g3.119.400970

921 74. Suk HY, Neff BD. Microsatellite genetic differentiation among populations of the
922 Trinidadian guppy. Heredity . 2009;102: 425–434.

923 75. Blondel L, Baillie L, Quinton J, Alemu JB, Paterson I, Hendry AP, et al. Evidence for
924 contemporary and historical gene flow between guppy populations in different
925 watersheds, with a test for associations with adaptive traits. Ecol Evol. 2019;10: 1.

926 76. Jones FC, Grabherr MG, Chan YF, Russell P, Mauceli E, Johnson J, et al. The genomic basis
927 of adaptive evolution in threespine sticklebacks. Nature. 2012;484: 55–61.

928 77. Lamichhaney S, Fuentes-Pardo AP, Rafati N, Ryman N, McCracken GR, Bourne C, et al.
929 Parallel adaptive evolution of geographically distant herring populations on both sides of
930 the North Atlantic Ocean. Proc Natl Acad Sci U S A. 2017;114: E3452–E3461.

931 78. Barrett RDH, Schluter D. Adaptation from standing genetic variation. Trends Ecol Evol.
932 2008;23: 38–44.

933 79. Cayuela H, Rougemont Q, Laporte M, Mérot C, Normandeau E, Dorant Y, et al. Shared
934 ancestral polymorphism and chromosomal rearrangements as potential drivers of local
935 adaptation in a marine fish. Mol Ecol. 2020. doi:10.1111/mec.15499

936 80. Lai Y-T, Yeung CKL, Omland KE, Pang E-L, Hao Y, Liao B-Y, et al. Standing genetic variation
937 as the predominant source for adaptation of a songbird. Proc Natl Acad Sci U S A.
938 2019;116: 2152–2157.

939 81. Conte GL, Arnegard ME, Peichel CL, Schluter D. The probability of genetic parallelism and
940 convergence in natural populations. Proc Biol Sci. 2012;279: 5039–5047.

941 82. Jacobs A, Carruthers M, Yurchenko A, Gordeeva NV, Alekseyev SS, Hooker O, et al.
942 Parallelism in eco-morphology and gene expression despite variable evolutionary and
943 genomic backgrounds in a Holarctic fish. PLoS Genet. 2020;16: e1008658.

944 83. Van Belleghem SM, Vangestel C, De Wolf K, De Corte Z, Möst M, Rastas P, et al. Evolution
945 at two time frames: Polymorphisms from an ancient singular divergence event fuel
946 contemporary parallel evolution. PLoS Genet. 2018;14: e1007796.

947 84. Maître J-L, Heisenberg C-P. Three functions of cadherins in cell adhesion. Curr Biol.
948 2013;23: R626–33.

949 85. Garcia de la Serrana D, Devlin RH, Johnston IA. RNAseq analysis of fast skeletal muscle in
950 restriction-fed transgenic coho salmon (Oncorhynchus kisutch): an experimental model
951 uncoupling the growth hormone and nutritional signals regulating growth. BMC Genomics.
952 2015;16: 564.

953 86. Zartman JJ, Kanodia JS, Yakoby N, Schafer X, Watson C, Schlichting K, et al. Expression
954 patterns of cadherin genes in Drosophila oogenesis. Gene Expr Patterns. 2009;9: 31–36.

955 87. Yeaman S, Whitlock MC. The genetic architecture of adaptation under migration-selection
956 balance. Evolution. 2011;65: 1897–1911.

957 88. Griswold CK. Gene flow's effect on the genetic architecture of a local adaptation and its
958 consequences for QTL analyses. Heredity . 2006;96: 445–453.

959 89. Feller AF, Haesler MP, Peichel CL, Seehausen O. Genetic architecture of a key reproductive
960 isolation trait differs between sympatric and non-sympatric sister species of Lake Victoria
961 cichlids. Proc Biol Sci. 2020;287: 20200270.

962 90. Browning BL, Zhou Y, Browning SR. A One-Penny Imputed Genome from Next-Generation
963 Reference Panels. Am J Hum Genet. 2018;103: 338–348.

964 91. Delaneau O, Zagury J-F, Marchini J. Improved whole-chromosome phasing for disease and
965 population genetic studies. Nat Methods. 2013;10: 5–6.

966 92. Malinsky M, Svardal H, Tyers AM, Miska EA, Genner MJ, Turner GF, et al. Whole-genome
967 sequences of Malawi cichlids reveal multiple radiations interconnected by gene flow. Nat
968 Ecol Evol. 2018;2: 1940–1955.

969 93. Danecek P, Auton A, Abecasis G, Albers CA, Banks E, DePristo MA, et al. The variant call
970 format and VCFtools. Bioinformatics. 2011;27: 2156–2158.

971 94. Bagley RK, Sousa VC, Niemiller ML, Linnen CR. History, geography and host use shape
972 genomewide patterns of genetic variation in the redheaded pine sawfly (Neodiprion
973 lecontei). Mol Ecol. 2017;26: 1022–1044.

974 95. Szpiech ZA, Hernandez RD. selscan: an efficient multithreaded program to perform EHH-
975 based scans for positive selection. Mol Biol Evol. 2014;31: 2824–2827.

976 96. Yates AD, Achuthan P, Akanni W, Allen J, Allen J, Alvarez-Jarreta J, et al. Ensembl 2020.
977 Nucleic Acids Res. 2020;48: D682–D688.

978 97. Thomas PD, Campbell MJ, Kejariwal A, Mi H, Karlak B, Daverman R, et al. PANTHER: a
979 library of protein families and subfamilies indexed by function. Genome Res. 2003;13:
980 2129–2141.

981 98. Layer RM, Chiang C, Quinlan AR, Hall IM. LUMPY: a probabilistic framework for structural
982 variant discovery. Genome Biol. 2014;15: R84.

983 99. Layer R. samplot: Plot structural variant signals from many BAMs and CRAMs. Github;
984 2020. Available: https://github.com/ryanlayer/samplot

985 100. Kozlov AM, Darriba D, Flouri T, Morel B, Stamatakis A. RAxML-NG: a fast, scalable and user-
986 friendly tool for maximum likelihood phylogenetic inference. Bioinformatics. 2019;35:
987 4453–4455.